

# Adaptive Growth of the Ductus Arteriosus and Aortic Isthmus in Various Ductus-Dependent Complex Congenital Heart Diseases

**Liza Hashim**

Nemours Children's Health

**Daniel Vari**

Nemours Children's Health

**Abdul M. Bhat**

Nemours Cardiac Center, Nemours Children's Health

**Takeshi Tsuda** (✉ [ttsuda@nemours.org](mailto:ttsuda@nemours.org))

Nemours Cardiac Center, Nemours Children's Health

---

## Research Article

**Keywords:** Embryonic aortic arch, Cardiovascular development, Brain sparing effects, Morphogenesis, Shear stress, Echocardiogram

**Posted Date:** May 8th, 2023

**DOI:** <https://doi.org/10.21203/rs.3.rs-2883826/v1>

**License:**  This work is licensed under a Creative Commons Attribution 4.0 International License.

[Read Full License](#)

**Additional Declarations:** No competing interests reported.

---

**Version of Record:** A version of this preprint was published at Pediatric Cardiology on July 21st, 2023. See the published version at <https://doi.org/10.1007/s00246-023-03236-4>.

# Abstract

**Background:** The ductus arteriosus (DA) is critical in maintaining postnatal circulation in neonates with obstructed systemic circulation (OSC) and pulmonary circulation (OPC). We hypothesized that the size of the DA and aortic isthmus (Aol) undergoes adaptive growth *in utero* to counteract the hemodynamic challenges in these congenital heart diseases (CHD).

**Methods:** Postnatal echocardiograms of neonates diagnosed prenatally with ductal-dependent CHD who were started on prostaglandins within 24 hours of birth were reviewed. We assessed the cross-sectional area of the aortic valve opening, pulmonary valve opening, Aol, and DA by calculating  $(\text{diameter})^2/\text{body surface area}$ . Neonates were classified into OSC or OPC then subgrouped depending upon the patency of semilunar valves: OSC with and without aortic atresia (OSC-AA and OSC-nAA, respectively) and OPC with and without pulmonary atresia (OPC-PA and OPC-nPA, respectively).

**Results:** Ninety-four cases were studied. The DA in OSC was significantly larger than OPC, and the DA in OSC-AA was significantly larger than OSC-nAA. The size of the Aol was significantly larger in OPC than OSC and larger in OSC-AA than OSC-nAA. Within the OSC-nAA group, there was no significant difference in the size of the DA, Aol, or pulmonary valve opening between those with retrograde flow (RF) at the Aol and without (nRF) except the aortic valve opening was significantly larger in nRF. All groups had comparable cross-sectional areas of systemic output.

**Conclusions:** Our findings suggest that DA and Aol show compensatory growth to maintain critical blood flow to vital organs against primary anatomical abnormalities in ductus-dependent CHD.

## 1. Introduction

The ductus arteriosus (DA) is an essential cardiovascular structure *in utero* that bypasses blood from the pulmonary trunk to the descending aorta (DAo) to perfuse the placenta and lower part of the body. After birth, pulmonary vascular resistance progressively declines with initiation of spontaneous breathing and increase in systemic oxygenation. Interruption of the placental circulation raises the systemic vascular resistance, resulting in further increase of pulmonary blood flow. This transition to neonatal circulation stimulates the DA to close spontaneously in conjunction with an increase in the size of the aortic isthmus (Aol) within the first couple of days after birth in normal term newborn infants [1].

The fetal DA and Aol play a critical role in maintaining normal blood flow in fetuses with and without complex congenital heart disease (CHD). In neonates with abnormalities of the left ventricular (LV) outflow tract, aortic arch, or both, there may be a potential compromise of circulation to vital fetal organs, especially to the brain. The adaptive growth of the DA and Aol would help overcome these hemodynamic challenges [2,3]. In CHD with obstructed systemic circulation (OSC), the postnatal DA (patent DA [PDA]) is markedly larger than in CHD with obstructed pulmonary circulation (OPC) because a large amount of systemic cardiac output is carried through the DA *in utero* [4]. It has been suggested that there is preferential redistribution of blood flow to the brain to deliver optimal cerebral oxygen supply in fetuses

with CHD [5,6]. These studies used a single Doppler measurement collected during the second or third trimester to estimate blood flow. However, some questions were raised regarding predicting accurate blood flow solely from Doppler measurements in fetuses with CHD [7].

We aimed to investigate whether fetal DA and Aol show compensatory growth to overcome hemodynamic challenges caused by primary structural abnormalities in PDA-dependent complex CHD to support optimum fetal growth. We tested this hypothesis by measuring the anatomical structure of the great arteries and ventricular outflow tracts in newborn infants prenatally diagnosed with PDA-dependent complex CHD with either OSC or OPC who were started on prostaglandin E1 (PGE1) infusion, which is used to maintain patency of the DA in CHD, within 24 hours of birth.

## 2. Methods

This study was approved by the Institutional Review Board of Nemours Children's Health, Wilmington, Delaware. We performed a retrospective chart review on neonates admitted to Nemours Cardiac Center with a diagnosis of CHD between January 1998 and December 2020. Primary inclusion criteria were neonates with prenatally diagnosed PDA-dependent CHD (OSC or OPC) who were started on a prostaglandin infusion within 24 hours after birth. We excluded any patients who did not have a PDA or an Aol (i.e., interrupted aortic arch) and those who did not have an echocardiogram within 24 hours after birth.

### 2.1 Demographic information

Demographic and clinical variables were gathered from the electronic medical record. These variables included sex, gestational age (prematurity was defined as less than 37 weeks of gestation), prenatal cardiac diagnosis and type of obstruction, weight, height, and body surface area at birth. Records reviewed included admission history and physical, birth records from referring hospitals, and digitally stored echocardiogram images and reports. Final cardiac diagnosis was obtained from initial echocardiographic reports, early postoperative notes, or both, when available.

### 2.2 Classifications

All included neonates had a primary cardiac diagnosis of PDA-dependent CHD with OSC or OPC. Multiple variants of OSC were subgrouped depending upon the presence or absence of aortic atresia (AA): with AA (OSC-AA) or without (n) AA (OSC-nAA). Hypoplastic left heart syndrome (HLHS) was defined as an underdeveloped LV structure with variable degrees of left-sided obstruction and/or aortic arch hypoplasia. Similarly, OPC was subgrouped by presence or absence of pulmonary atresia (PA): with PA (OPC-PA) or without PA (OPC-nPA).

### 2.3 Echocardiographic analysis

By two-dimensional echocardiogram and color Doppler images, diameters of various vessels and valve openings were measured. These measurements included aortic valve opening (AVO), pulmonary valve

opening (PVO), DA, and Aol in three different views. To ensure accuracy, echocardiographic measurements were performed independently by three different examiners (LH, AMB, and TT). Three measurements were collected at peak systole, and then the mean was obtained. The AVO and PVO were measured in the parasternal long axis view. In the parasternal short axis and suprasternal views, the diameter of the DA was measured at the narrowest section. The Aol was measured in the suprasternal view. With color Doppler images, the presence of diastolic retrograde flow across Aol was examined. Cross-sectional areas of vascular structures (PDA and Aol) and semilunar valve openings (AVO and PVO) were represented by squaring a measured diameter (mm<sup>2</sup>) indexed to the body surface area (BSA; m<sup>2</sup>). Body surface area was obtained by Haycock formula: BSA (m<sup>2</sup>) = weight (kg)<sup>0.5378</sup> x height (cm)<sup>0.3964</sup> x 0.024265. The cross-sectional area was considered a marker of the estimated flow passing across the specific site. Thus, systemic blood flow was estimated utilizing the following formulas for each category of lesion:

$$\text{OSC: } (\text{AVO})^2/\text{BSA} + (\text{PDA})^2/\text{BSA}$$

$$\text{OPC: } (\text{AVO})^2/\text{BSA} - (\text{PDA})^2/\text{BSA}$$

Unit: mm<sup>2</sup>/BSA (m<sup>2</sup>)

By color Doppler study across Aol, OSC-nAA was further divided into those with retrograde flow (RF) across the Aol (nAA-RF) and those without (nAA-nRF).

## 2.4 Statistics

All variables were reported as mean  $\pm$  standard deviation. A one-way analysis of variance was conducted to evaluate the difference among the means of multiple groups and subgroups. GraphPad Prism 6 (GraphPad, San Diego, CA, USA) was the statistical package used for further analysis. Tukey's multiple comparison test was generated to assess which of the means were different. The results yielded an adjusted *p* value, and a *p* value of < 0.05 was considered statistically significant.

## 3. Results

Ninety-four neonates met primary inclusion criteria: 60 neonates with OSC and 34 with OPC (**Table 1**). Within the OSC group, 10 patients had AA (OSC-AA), and 50 patients had a non-atretic aortic valve (OSC-nAA). In the OSC-nAA group, 32 patients had coarctation of the aorta (CoA) with aortic arch hypoplasia (14 RF and 18 nRF), 11 had HLHS (9 RF and 2 nRF), 3 had critical aortic stenosis (AS) (all RF), and 4 had severely unbalanced complete common atrioventricular canal (CCAVC; HLHS variant) (all RF). In neonates with OPC, 19 patients had PA (OPC-PA), and 15 had a non-atretic pulmonary valve (OPC-nPA). Associated cardiac anomalies included tetralogy of Fallot (TOF), double-outlet right ventricle (DORV) with pulmonary stenosis, PA with intact ventricular septum, critical valvar pulmonary stenosis, tricuspid atresia, and Ebstein's anomaly (**Table 1**).

The patients' baseline characteristics including gestational age, sex, birth weight, and BSA were comparable across the four subgroups (OSC-AA, OSC-nAA, OPC-PA, and OPC-nPA) and between nAA-RF and nAA-nRF (**Table 2**).

The cross-sectional areas of key anatomical structures are shown in **Figure 1**. The AVO was significantly larger in the OPC groups (OPC-PA:  $323 \pm 83 \text{ mm}^2/\text{m}^2$ , OPC-nPA:  $306 \pm 105 \text{ mm}^2/\text{m}^2$ ) than OSC (OSC-AA: 0, OSC-nAA:  $102 \pm 53 \text{ mm}^2/\text{m}^2$ ) ( $p < 0.0001$ ). The difference between OPC-PA and OPC-nPA was not statistically significant. The PVO was significantly larger in OSC (OSC-AA:  $373 \pm 103 \text{ mm}^2/\text{m}^2$ , OSC-nAA:  $341 \pm 80 \text{ mm}^2/\text{m}^2$ ) than in OPC (OPC-PA: 0, OPC-nPA:  $36 \pm 13 \text{ mm}^2/\text{m}^2$ ) ( $p < 0.0001$ ). There was no significant difference in PVO between OSC-AA and OSC-nAA. The cross-sectional area of the PDA was largest in OSC-AA ( $255 \pm 63 \text{ mm}^2/\text{m}^2$ ) and significantly larger than OSC-nAA ( $152 \pm 38 \text{ mm}^2/\text{m}^2$ ), OPC-PA ( $67 \pm 20 \text{ mm}^2/\text{m}^2$ ), or OPC-nPA ( $64 \pm 20 \text{ mm}^2/\text{m}^2$ ) (all  $p < 0.0001$ ). The PDA in OSC-nAA ( $152 \pm 38 \text{ mm}^2/\text{m}^2$ ) was also significantly larger than that of both OPC-PA and OPC-nPA ( $p < 0.0001$ ). The Aol was larger in OPC groups (OPC-PA:  $206 \pm 56 \text{ mm}^2/\text{m}^2$  and OPC-nPA:  $178 \pm 46 \text{ mm}^2/\text{m}^2$ ) versus OSC groups (OSC-AA:  $125 \pm 51 \text{ mm}^2/\text{m}^2$  and OSC-nAA:  $29 \pm 16 \text{ mm}^2/\text{m}^2$ ) ( $p < 0.005$ ). The cross-sectional areas of total systemic output, a sum of systemic and pulmonary blood flow, were comparable in all 4 groups with no statistically significant difference.

We further investigated the cross-sectional areas within the OSC cohort (**Figure 2**). The AVO was significantly larger in nAA-nRF than in nAA-RF ( $p < 0.0044$ ), suggesting that the presence of retrograde Aol flow was associated with lower antegrade flow across the aortic valve. There was no significant difference in PVO among these 3 subgroups. The PDA sizes were the largest in the OSC-AA group ( $255 \pm 63 \text{ mm}^2/\text{m}^2$ ) when compared with nAA-RF ( $154 \pm 34 \text{ mm}^2/\text{m}^2$ ) or nAA-nRF ( $148 \pm 44 \text{ mm}^2/\text{m}^2$ ) ( $p < 0.0001$ ), while there was no significant difference between nAA-RF and nAA-nRF ( $p = 0.8489$ ). The size of the Aol was significantly larger in the OSC-AA group ( $125 \pm 51 \text{ mm}^2/\text{m}^2$ ) than in nAA-RF ( $33 \pm 20 \text{ mm}^2/\text{m}^2$ ) or nAA-nRF ( $26 \pm 12 \text{ mm}^2/\text{m}^2$ ) (both  $p < 0.0001$ ). Systemic output was comparable among these subgroups within OSC.

## 4. Discussion

Our findings suggest that there is adaptive growth of the DA and Aol *in utero* that may facilitate critical blood flow to vital organs in neonates with primary obstruction of systemic or pulmonary circulation. This concept was, in part, demonstrated in the chick embryo model [8,9] and fetal lamb studies [4,10]. A similar mechanism has been implicated in human fetuses [2]. This regulatory role of the DA and Aol was also demonstrated in anatomically normal late fetal circulation with pulse Doppler measurement in human fetuses [3,11]. We postulate that relative antegrade blood flow largely determines the size of cross-sectional areas of certain vascular structures including DA and Aol in ductus-dependent complex CHD. Through assessing relative cross-sectional areas of valve orifices and vascular structures soon after birth under PGE1 infusion, we were able to demonstrate that the DA in concert with Aol undergoes adaptive

growth to overcome the hemodynamic obstacles induced by primary cardiovascular structural abnormalities.

#### 4.1 What regulates the size of fetal vascular structure

Final cardiovascular morphology in OSC or OPC may be determined by both genetically regulated primary morphogenesis and secondary hemodynamic effects [12]. Abnormal genetic programming, subsequent signal transduction in the second heart field, and altered neural crest migration are known to cause primary structural abnormalities in the conotruncus and aortic arch vessels [13,14]. While genetic predisposition that regulates organized cell proliferation, differentiation, and migration contributes to the morphogenesis of outflow tracts and great vessels, wall shear stress may play a dominant role in regression, persistence, or growth of the original pharyngeal arches, as demonstrated in chick embryos [15]. Flow-induced morphological growth of a vascular structure is an important determinant in regulating the size of the structure to provide sufficient perfusion to meet the metabolic demand of the fetus [16,17].

The relative size of the AVO, DA, and DAo may reflect the amount of combined cardiac output these vessels support. Heyman and Rudolph demonstrated this principle in their study of term and preterm infants without CHD [18]. In structurally abnormal hearts, adaptive alterations in patterns of blood flow must occur to support the developing fetus. For example, in OSC, the DA provides most of combined cardiac output, resulting in the largest PDA size after birth. In cases of OPC, the LV carries virtually all the combined cardiac output, by which the development and caliber of aortic valve, ascending aorta, and Aol are significantly enlarged.

The DA is a unique muscular arterial vessel arranged in spiral and longitudinal layers with its patency heavily dependent on PGE where PGE-induced impaired elastogenesis inhibits its evolution to an elastic artery [19]. Neural crest cells differentiate into vascular smooth muscle cells of aortic arch vessels in a site-dependent fashion. Bergwerff et al. demonstrated that the DA, the derivative of the sixth embryonic arch, receives an extensive neural crest contribution but does not join the other arch derivatives in their elastogenetic differentiation [20]. In contrast, the Aol is a part of the aorta consisting of multilayers of elastin lamina distinct from the DA, and its patency is independent of PGE. The Aol originates from the fourth embryonic arch and was shown to reveal unique features of vascular structure distinct from the rest of the aortic arch components in the mouse model, which helps us understand the pathogenesis of interrupted aortic arch and aberrant subclavian artery [21]. It is intriguing to see the similar purposeful flexibility of DA and Aol in fetal development despite their different embryonic background and histological features. The underlying regulatory mechanisms that regulate collaborative growth of DA and Aol are yet to be elucidated.

#### 4.2 Combinational adaptive growth of DA and Aol

In OPC, the LV provides most of the systemic cardiac output (both brachiocephalic and placental circulation), whereas the DA exclusively serves as a conduit to perfuse the lungs that receive no more than 20% of the combined cardiac output in humans (approximately 8 to 10% of combined cardiac

output in fetal lambs) [4]. In contrast, in OSC, the right ventricle bears the responsibility of supporting most of the systemic circulation via the DA, including placental flow [22]. This increased output produces a larger-caliber DA, consistent with our current data. Moreover, we demonstrated that patients with less severe aortic valve obstruction (i.e., OSC-nAA) did not require the DA to accommodate as much flow as OSC-AA. Hence, the DA was noted to be smaller, while a larger DA was seen in AA (OSC-AA) (**Figure 1**).

Similarly, we expect the caliber of the Aol to increase when it accommodates increased blood flow in cases of LV outflow tract obstruction. Normally, the LV ejects an estimated 40-50% of the combined ventricular output, but only 10% of that traverses the Aol to the DAo, while the rest is directed to the head and neck vessels [4]. When there is complete obstruction of the LV output, the head and neck vessels are exclusively supplied by RF across the Aol. As the degree of LV outflow tract obstruction increases, more RF across the Aol is required. When we assessed the size and caliber of the Aol, infants with AA (OSC-AA) had a larger Aol compared with those with non-atretic aortic valves (OSC-nAA) (**Figure1**). In OSC patients, presence of RF across Aol was associated with smaller AVO (**Figure 2**), suggesting adaptive growth of Aol to maintain sufficient brain perfusion that would have been otherwise compromised by a severely restricted antegrade flow across the aortic valve (no antegrade flow in OSC-AA). Fetal Aol plays an important regulatory role as an arterial watershed between brachiocephalic and subdiaphragmatic circulations [11,23].

#### 4.3 Brain-sparing effect as a critical regulatory factor

In utero, the fetal brain is very sensitive to hypoxia and thus induces a “brain-sparing phenomenon” to ensure its optimum growth [24-26]. By this mechanism, fetal blood flow is redistributed away from peripheral vasculature and prioritized toward an essential circulation through direct vasodilatation of the cerebral vascular bed and simultaneous peripheral vasoconstriction [25,27], allowing an RF across Aol with [4] and without CHD [3]. With CHD, especially in OSC, critical hemodynamic alterations occur *in utero* and lead to these changes [28,29]. Adaptive growth of the DA and Aol is attributed to the increased blood flow following the decrease in cerebral vascular impedance, a critical process in preserving cerebral oxygen delivery in complex CHD [6,30] similar to the mechanisms of cerebral hemodynamic adaptation seen in fetuses with placental insufficiency. We speculate that autoregulation of cerebral circulation in utero is a primary determinant of the secondary adaptative growth of the DA and Aol. This principle was demonstrated in our study of patients comparing OSC-AA with OSC-nAA groups and nAA-RF with nAA-nRF groups.

#### 4.4 Limitations

We acknowledge certain limitations in this study. First, the circulatory model in this study, an early neonatal circulation under PGE1 infusion, is different from late gestational fetal circulation because of postnatal changes resulting in increase in pulmonary blood flow due to lowered pulmonary vascular resistance and an absence of the placenta. However, we postulated this model is similar to the late gestational fetal environment while acknowledging these differences. Second, we measured total cross-sectional areas to estimate the amount of blood flow passing across the specific structures of interest,

not the flow itself. In addition, we represented cross-sectional areas by (diameter)<sup>2</sup> of the structure, assuming all cross-sectional areas are round. In fact, some may be of an oval shape. Flow is also influenced by impedance of distal vasculature and viscosity of blood, which were not examined in this study. Lastly, this is a retrospective study with a small size of 94 patients, limiting the power of this investigation.

## 5. Conclusion

Fetuses can survive to term despite abnormal cardiovascular anatomy in complex CHD as they are supported by secondary adaptive changes in the DA and AoI to ensure necessary perfusion to growing vital organs and placenta. With certain critical regulatory mechanisms, the size and morphology of the DA and AoI grow in accordance with essential metabolic demand to deliver oxygen and nutrients to the fetus, especially to the developing brain. This study provides a proof of evidence that cooperative adaptive growth of the DA and AoI counteracts hemodynamic challenges induced by primary structural abnormalities as previously proposed [3,7,11,30]. The combination of primary morphological anomalies and secondary adaptive responses determines the overall cardiovascular phenotype supporting the growing fetus and fetal life. Further investigation is required to identify how biomechanical factors and gene expressions interact to direct cardiac morphogenesis.

## Abbreviations

AA (Aortic atresia), AoI (Aortic isthmus), AS (Aortic stenosis), AVO (Aortic valve opening), BSA (Body surface area), CoA (Coarctation of aorta), CCAVC (Complete common atrioventricular canal), CHD (Congenital heart disease), DA (Ductus arteriosus), DAo (Descending aorta), DORV (Double outlet right ventricle), HLHS (Hypoplastic left heart syndrome), IVS (Intact ventricular septum), LV (left ventricle/ventricular), MA (Mitral Atresia), MS (Mitral stenosis), n (Without), OPC (Obstructed pulmonary circulation), OSC (Obstructed systemic circulation), PA (Pulmonary atresia), PDA (Patent ductus arteriosus), PGE1 (Prostaglandin E1), PS (Pulmonary stenosis), PVO (Pulmonary valve opening), RF (Retrograde flow), TOF (tetralogy of Fallot)

## Declarations

Authors have no financial or non-financial interests that are directly or indirectly related the work submitted for the publication. This research did not receive any specific grant from funding agencies in the public, commercial, or not-for-profit sectors.

## Author Contributions

TT conceptualized the study design. All authors participated in data collection. LH, AMB, and TT analyzed the collected data, and LH and TT summarized the data and created the Tables and Figures. LH



wrote an original draft, which was repeatedly edited by TT and AMB. All authors reviewed and approved the final version of the manuscript.

## Acknowledgement

We thank Ms. Kimberley Eissmann for her editing of the manuscript text.

## References

1. Machii M, Becker AE (1997) Morphologic features of the normal aortic arch in neonates, infants, and children pertinent to growth. *Ann Thorac Surg* 64:511–515
2. Rudolph AM, Heymann MA, Spitznas U (1972) Hemodynamic considerations in the development of narrowing of the aorta. *Am J Cardiol* 30:514–525
3. Tynan D, Alphonse J, Henry A, Welsh AW (2016) The Aortic Isthmus: A Significant yet Underexplored Watershed of the Fetal Circulation. *Fetal Diagn Ther* 40:81–93
4. Rudolph AM (2010) Congenital cardiovascular malformations and the fetal circulation. *Arch Dis Child Fetal Neonatal Ed* 95:F132–136
5. Ruiz A, Cruz-Lemini M, Masoller N, Sanz-Cortes M, Ferrer Q, Ribera I, Martinez JM, Crispi F, Arevalo S, Gomez O, Perez-Hoyos S, Carreras E, Gratacos E, Llurba E (2017) Longitudinal changes in fetal biometry and cerebroplacental hemodynamics in fetuses with congenital heart disease. *Ultrasound Obstet Gynecol* 49:379–386
6. Hahn E, Szwasz A, Cnota J 2nd, Levine JC, Fifer CG, Jaeggi E, Andrews H, Williams IA (2016) Association between fetal growth, cerebral blood flow and neurodevelopmental outcome in univentricular fetuses. *Ultrasound Obstet Gynecol* 47:460–465
7. Mebius MJ, Clur SAB, Vink AS, Pajkrt E, Kalteren WS, Kooi EMW, Bos AF, du, Sarvaas M, Bilardo GJ (eds) (2019) CM Growth patterns and cerebroplacental hemodynamics in fetuses with congenital heart disease. *Ultrasound Obstet Gynecol* 53: 769–778
8. Kowalski WJ, Dur O, Wang Y, Patrick MJ, Tinney JP, Keller BB, Pekkan K (2013) Critical transitions in early embryonic aortic arch patterning and hemodynamics. *PLoS ONE* 8:e60271
9. Lindsey SE, Menon PG, Kowalski WJ, Shekhar A, Yalcin HC, Nishimura N, Schaffer CB, Butcher JT, Pekkan K (2015) Growth and hemodynamics after early embryonic aortic arch occlusion. *Biomech Model Mechanobiol* 14:735–751
10. Rudolph AM, Heymann MA (1970) Circulatory changes during growth in the fetal lamb. *Circ Res* 26:289–299
11. Fouron JC (2003) The unrecognized physiological and clinical significance of the fetal aortic isthmus. *Ultrasound Obstet Gynecol* 22:441–447

12. Kowalski WJ, Pekkan K, Tinney JP, Keller BB (2014) Investigating developmental cardiovascular biomechanics and the origins of congenital heart defects. *Front Physiol* 5:408
13. Kelly RG (2012) The second heart field. *Curr Top Dev Biol* 100:33–65
14. Jiang X, Rowitch DH, Soriano P, McMahon AP, Sucov HM (2000) Fate of the mammalian cardiac neural crest. *Development* 127:1607–1616
15. Wang Y, Dur O, Patrick MJ, Tinney JP, Tobita K, Keller BB, Pekkan K (2009) Aortic arch morphogenesis and flow modeling in the chick embryo. *Ann Biomed Eng* 37:1069–1081
16. Lindsey SE, Butcher JT, Yalcin HC (2014) Mechanical regulation of cardiac development. *Front Physiol* 5:318
17. De Mey JG, Schiffers PM, Hilgers RH, Sanders MM (2005) Toward functional genomics of flow-induced outward remodeling of resistance arteries. *Am J Physiol Heart Circ Physiol* 288:H1022–1027
18. Heymann MA, Rudolph AM (1972) Effects of congenital heart disease on fetal and neonatal circulations. *Prog Cardiovasc Dis* 15:115–143
19. Yokoyama U, Ichikawa Y, Minamisawa S, Ishikawa Y (2017) Pathology and molecular mechanisms of coarctation of the aorta and its association with the ductus arteriosus. *J Physiol Sci* 67:259–270
20. Bergwerff M, Verberne ME, DeRuiter MC, Poelmann RE, Gittenberger-de Groot AC (1998) Neural crest cell contribution to the developing circulatory system: implications for vascular morphology? *Circ Res* 82:221–231
21. Bergwerff M, DeRuiter MC, Hall S, Poelmann RE, Gittenberger-de Groot AC (1999) Unique vascular morphology of the fourth aortic arches: possible implications for pathogenesis of type-B aortic arch interruption and anomalous right subclavian artery. *Cardiovasc Res* 44:185–196
22. Friedman AH, Fahey JT (1993) The transition from fetal to neonatal circulation: normal responses and implications for infants with heart disease. *Semin Perinatol* 17:106–121
23. Kiserud T, Acharya G (2004) The fetal circulation. *Prenat Diagn* 24:1049–1059
24. Donofrio MT, Bremer YA, Schieken RM, Gennings C, Morton LD, Eidem BW, Cetta F, Falkensammer CB, Huhta JC, Kleinman CS (2003) Autoregulation of cerebral blood flow in fetuses with congenital heart disease: the brain sparing effect. *Pediatr Cardiol* 24:436–443
25. Giussani DA (2016) The fetal brain sparing response to hypoxia: physiological mechanisms. *J Physiol* 594:1215–1230
26. Giussani DA, Davidge ST (2013) Developmental programming of cardiovascular disease by prenatal hypoxia. *J Dev Orig Health Dis* 4:328–337
27. Cohn HE, Sacks EJ, Heymann MA, Rudolph AM (1974) Cardiovascular responses to hypoxemia and acidemia in fetal lambs. *Am J Obstet Gynecol* 120:817–824
28. Modena A, Horan C, Visintine J, Chanthasenanont A, Wood D, Weiner S (2006) Fetuses with congenital heart disease demonstrate signs of decreased cerebral impedance. *Am J Obstet Gynecol* 195:706–710

29. Kaltman JR, Di H, Tian Z, Rychik J (2005) Impact of congenital heart disease on cerebrovascular blood flow dynamics in the fetus. *Ultrasound Obstet Gynecol* 25:32–36
30. Arduini M, Rosati P, Caforio L, Guariglia L, Clerici G, Di Renzo GC, Scambia G (2011) Cerebral blood flow autoregulation and congenital heart disease: possible causes of abnormal prenatal neurologic development. *J Matern Fetal Neonatal Med* 24:1208–1211

## Tables

**Table 1** Baseline Congenital Heart Disease of the Patients

I.	<b>Obstructed Systemic Circulation (OSC)</b>	<b>60</b>
	<b>Aortic Atresia (OSC-AA)</b>	<b>10</b>
	HLHS (MA)	9
	HLHS (MS)	1
	<b>Non-Aortic Atresia (OSC-nAA)</b>	<b>50</b>
RF	Retrograde Flow across AoI	30
	CoA/Arch Hypoplasia	14
	HLHS (AS)	9
	Critical AS	3
	Unbalanced CCAVC	4
nRF	No Retrograde Flow across AoI	20
	CoA/Arch Hypoplasia	18
	HLHS (AS)	2
II.	<b>Obstructed Pulmonary Circulation (OPC)</b>	<b>34</b>
	<b>Pulmonary Atresia (OPC-PA)</b>	<b>19</b>
	PA/IVS	7
	TOF/PA	3
	DORV/PA	3
	Ebstein's Anomaly/PA	2
	Tricuspid Atresia/PA	2
	Other with PA	2
	<b>Non-Pulmonary Atresia (OPC-nPA)</b>	<b>15</b>
	Critical Valvar PS	6
	TOF	4
	DORV	3
	Ebstein's Anomaly	1
	Other	1

HLHS; hypoplastic left heart syndrome, AA: aortic atresia, MA: mitral atresia, MS: mitral stenosis, nAA: non-aortic atresia, RF: retrograde flow, AoI: aortic isthmus, CoA: coarctation of aorta, PA/IVS; pulmonary atresia with intact ventricular septum, TOF; tetralogy of Fallot, PA; pulmonary atresia, DORV; double outlet right ventricle.

**Table 2** Demographic Information of Sub-Grouped Patients

	OSC-AA	OSC-nAA	nAA-RF	nAA-nRF	OPC-PA	OPC-nPA
Number	10	50	30	20	19	15
GA (weeks)	38.3 ± 0.8	38.0 ± 1.9	37.8 ± 2.2	38.4 ± 1.2	37.0 ± 2.9	38.6 ± 1.0
Sex (M/F)	5/5	24/26	15/15	9/11	9/10	8/7
BW (kg)	3.0 ± 0.4	3.0 ± 0.7	3.0 ± 0.8	3.1 ± 0.7	2.6 ± 0.8	3.3 ± 0.5
BSA (m <sup>2</sup> )	0.19 ± 0.01	0.19 ± 0.03	0.19 ± 0.03	0.19 ± 0.04	0.17 ± 0.04	0.20 ± 0.02

AA, aortic atresia; BSA, body surface area; BW, birth weight; F, female; GA, gestational age; M, male; nAA, non-aortic atresia; nPA, non-pulmonary atresia; nRF, non-retrograde flow; OPC, obstructed pulmonary circulation; OSC, obstructed systemic circulation; PA, pulmonary atresia; RF, retrograde flow.

## Figures

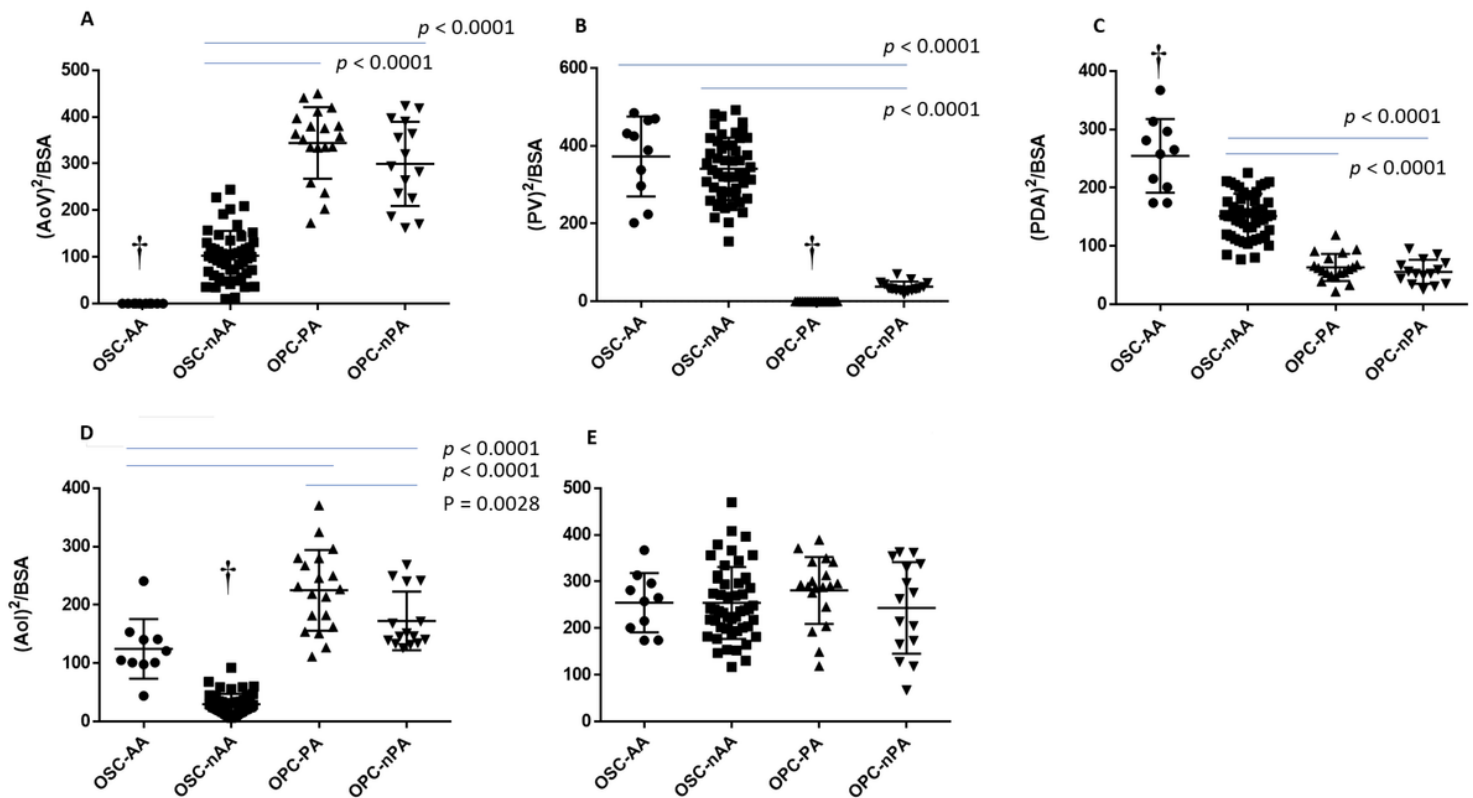


**Figure 1**

Cross-sectional areas of **A**: aortic valve opening (AVO), **B**: pulmonary valve opening (PVO), **C**: patent ductus arteriosus (PDA), **D**: aortic isthmus (AoI), and **E**: total systemic output in obstructed systemic circulation (OSC) with aortic atresia (AA) and without AA (nAA) and obstructed pulmonary circulation

(OPC) with pulmonary atresia (PA) and without PA (nPA). †Implies that the indicated group is significantly different from the other 3 groups ( $p < 0.0001$ ). Total systemic flow was comparable among all groups (E). BSA, body surface area.

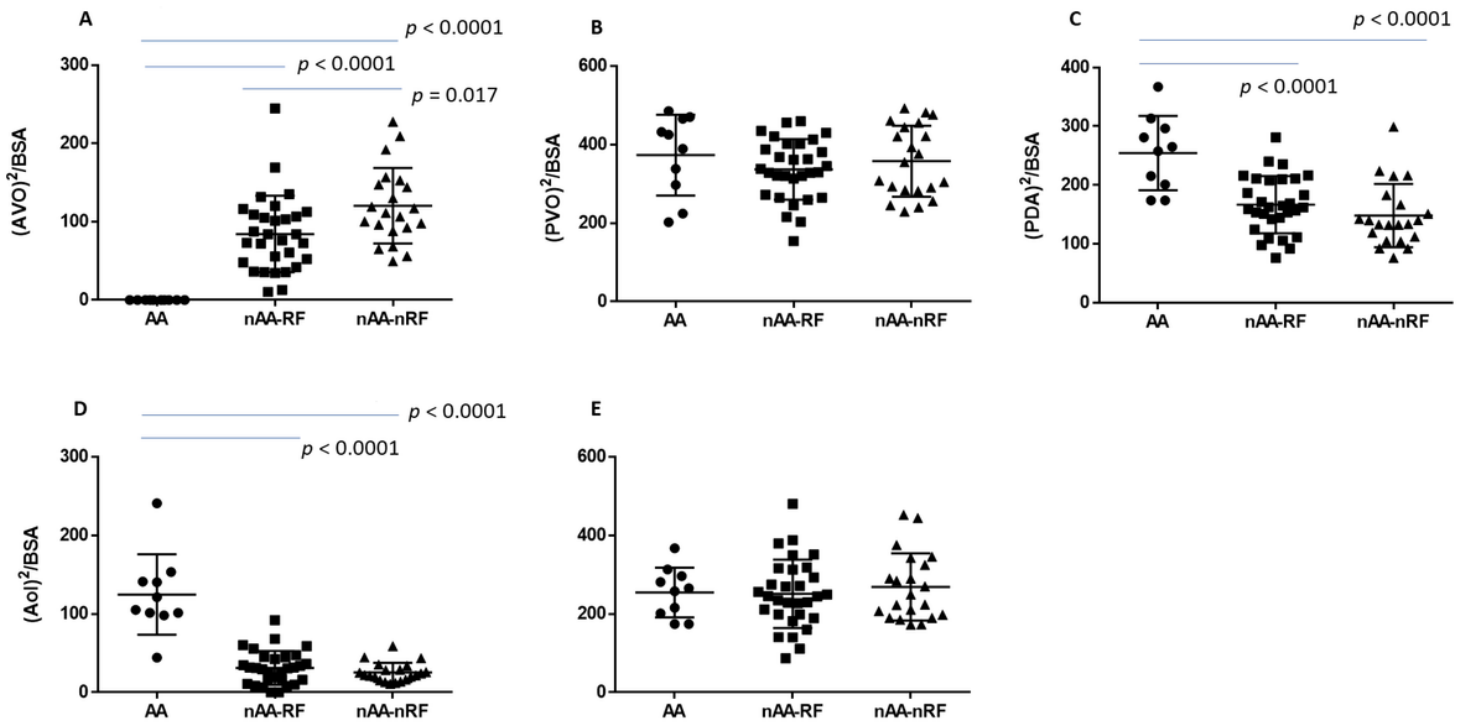


**Figure 2**

Cross-sectional areas of **A**: aortic valve opening (AVO), **B**: pulmonary valve opening (PVO), **C**: patent ductus arteriosus (PDA), **D**: aortic isthmus (Aoi), and **E**: total systemic output in obstructed systemic circulation (OSC) with variable degrees of aortic valve obstruction; aortic atresia (AA), non-AA with retrograde flow (nAA-RF) and without RF across the aortic isthmus (nAA-nRF). Between nAA-RF and nAA-nRF, there was a significant difference in AVO but no significant difference in the remaining parameters. Total systemic flow was comparable among the 3 groups (E). BSA, body surface area.